Journal of Solid State Chemistry 184 (2011) 1740–1748

Contents lists available at ScienceDirect

Journal of Solid State Chemistry

journal homepage: www.elsevier.com/locate/jssc

Rare configuration of tautomeric benzimidazolecarboxylate ligands in cadmium(II) and copper(II) coordination polymers

Jing-Yun Wu [a], Ciao-Wei Yang [a,b], Hui-Fang Chen [a,b], Yu-Chen Jao [a,c], Sheng-Ming Huang [a], Chiitang Tsai [b], Tien-Wen Tseng [c], Gene-Hsiang Lee [d], Shie-Ming Peng [d], Kuang-Lieh Lu [a,*]

[a] Institute of Chemistry, Academia Sinica, Taipei 115, Taiwan
[b] Department of Chemistry, Chinese Culture University, Taipei 111, Taiwan
[c] Department of Chemical Engineering, National Taipei University of Technology, Taipei 106, Taiwan
[d] Department of Chemistry, National Taiwan University, Taipei 107, Taiwan

ARTICLE INFO

Article history:
Received 30 September 2010
Received in revised form
26 April 2011
Accepted 1 May 2011
Available online 11 May 2011

Keywords:
Cadmium
Coordination polymer
Copper
Self-assembly

ABSTRACT

Two Cd(HBimc)-based isomers, $[Cd(HBimc^N)(HBimc^T)(H_2O)]\cdot 3.5H_2O\cdot EtOH$ (**1a**$\cdot 3.5H_2O\cdot EtOH$, H_2Bimc=1*H*-benzimidazole-5-carboxylic acid) and $[Cd(HBimc^N)(HBimc^T)(H_2O)]$ (**1b**), and two Cu(HMBimc)-based coordination polymers, $[Cu(HMBimc^N)_2(H_2O)]\cdot 1/2H_2O$ (**2**$\cdot 1/2H_2O$, H_2MBimc=2-methyl-1*H*-benzimidazole-5-carboxylic acid) and $[Cu(HMBimc^T)_2]\cdot 2THF\cdot H_2O$ (**3**$\cdot 2THF\cdot H_2O$), were self-assembled from $Cd(ClO_4)_2\cdot 6H_2O/H_2Bimc$ and $Cu(ClO_4)_2\cdot 6H_2O/H_2MBimc$ systems, respectively. Compound **1a** adopts a ladder-like chain structure, comprised of a hydrogen-bond-stabilized $Cd_2(HBimc^N)_2$-metallocyclic stair and a 1D straight $-(Cd-HBimc^T)_n-$ edge, whereas compound **1b** exhibits a 2D (4,4)-rhombus layered structure, intercrossed by 1D $-(Cd-HBimc^N)_n-$ chains and $-(Cd-HBimc^T)_n-$ chains. Compound **2** shows a 1D double-stranded wave-like chain from two single-stranded wave-like $-(Cu-HMBimc^N)_n-$ chains and compound **3** adopts a 2D (4,4)-topological layer structure, intercrossed by subunits of 1D $-(Cu-HMBimc^T)_n-$ chains. Interestingly, a pair of tautomeric HBimc building blocks—normal (*N* or $HBimc^N$) and tautomer (*T* or $HBimc^T$)—is simultaneously included in the structures of **1a** and **1b**, whilst the ***N***- and ***T***-configured HMBimc building blocks are present as separate entities in Cu species, **2** and **3**, respectively. The existence of only a tautomer (***T***) mode of the benzimidazolecarboxylate-based ligand in a Cu(II) network is observed for the first time.

1. Introduction

Research related to metal–organic framework (MOF) materials has been a subject of great interest, not only from the standpoint of the potential applications, but also because of their intriguing architectures and framework topologies [1–4]. The key to the successful design of a MOF material is the judicious selection of the molecular building blocks [2]. Among the many coordination ligands, imidazolecarboxylate is unique, in that it has a combination of flexible, multi-dentate, and asymmetric characteristics [5–18]. One of the features of this ligand is that it can exist in two resonated tautomeric forms, namely normal (***N***) and tautomer (***T***) configurations, which differ only in the position of a proton (Scheme 1) [15–17,19]. This has ramifications for the preparation of proton conducting materials and applications to fuel cell technology [20]. Considering its tautomeric nature, proton transfer capability, asymmetric multi-dentate geometry, and thermal stability, there is a great deal of fundamental coordination chemistry to learn from this compound. However, to our surprise, fundamental studies dealing with the coordination modes of these ligands in coordination compounds are limited.

Herein we report on some intriguing coordination modes of imidazolecarboxylates in four new MOFs constructed using either 1*H*-benzimidazole-5-carboxylate (HBimc) or 2-methyl-1*H*-benzimidazole-5-carboxylate (HMBimc) as building blocks. Interestingly, these results demonstrate unusual cases in which two different tautomeric HBimc building blocks (normal (***N***) and tautomer (***T***)) are simultaneously present in two Cd(HBimc)-based networks, whereas, the normal and tautomer modes of HMBimc are present in separate forms in two Cu(HMBimc)-based frameworks. The isolation of a metal–organic network containing only the tautomer (***T***) mode of the tautomeric benzimidazolecarboxylate-based ligand is reported for the first time.

2. Experimental section

2.1. General remarks

Chemical reagents were purchased commercially and were used as received without further purification. Thermogravimetric (TG) analyses were performed under nitrogen with a Perkin-Elmer

* Corresponding author. Fax: +886 2 27831237.
E-mail address: lu@chem.sinica.edu.tw (K.-L. Lu).

0022-4596/$ - see front matter © 2011 Elsevier Inc. All rights reserved.
doi:10.1016/j.jssc.2011.05.002

TGA-7 TG analyzer. Elemental analyses were conducted on a Perkin-Elmer 2400 CHN elemental analyzer.

2.2. Synthesis of $[Cd(HBimc^N)(HBimc^T)(H_2O)]\cdot 3.5H_2O\cdot EtOH$ (**1a**$\cdot 3.5H_2O\cdot EtOH$)

A solution of $Cd(ClO_4)_2\cdot 6H_2O$ (41.9 mg, 0.10 mmol) in EtOH (5 mL) was slowly layered on top of a mixture of EtOH and H_2O (1:1, 8 mL, middle), and an aqueous solution (5 mL, bottom) of H_2Bimc (17.8 mg, 0.11 mmol) and KOH (0.5 M) (pH=11–12). Colorless crystals (7.6 mg, 1.35×10^{-2} mmol), obtained after the mixture was kept several days without stirring at 4 °C, were collected in 24% yield. Anal. Calcd. for $C_{16}H_{19}CdN_4O_{8.5}$: C, 37.26; H, 3.71; N, 10.86%. Found: C, 37.55; H, 3.79; N, 10.73%.

2.3. Synthesis of $[Cd(HBimc^N)(HBimc^T)(H_2O)]$ (**1b**)

A mixture of $CdCl_2\cdot 2.5H_2O$ (23.8 mg, 0.10 mmol), H_2Bimc (81.3 mg, 0.50 mmol), and 1,4-diaza-bicyclo[2.2.2]octane (56.9 mg, 0.51 mmol) in an aqueous solution (5 mL, pH=8–9) was conducted in an acid digestion bomb at 150 °C for 72 h. Brown-colored crystals (40.6 mg, 8.97×10^{-2} mmol) were obtained and collected in 90% yield by filtration and washed with ethanol, and then dried at room temperature. Anal. Calcd. for $C_{16}H_{12}CdN_4O_5$: C, 42.45; H, 2.67; N, 12.38%. Found: C, 42.14; H, 2.48; N, 12.36%.

Scheme 1. Schematic representation of normal (***N***) and tautomer (***T***) forms of HBimc (R=H) and HMBimc (R=Me) ligand structures. Coordination sites and possible hydrogen-bonding donor–acceptor sites are indicated.

2.4. Synthesis of $[Cu(HMBimc^N)_2(H_2O)]\cdot 1/2H_2O$ (**2**$\cdot 1/2H_2O$)

A solution of $Cu(ClO_4)_2\cdot 6H_2O$ (74.2 mg, 0.20 mmol) in EtOH (5 mL) was slowly layered on top of THF (5 mL, middle), and an aqueous solution (5 mL, bottom) of H_2MBimc (88.1 mg, 0.50 mmol) and KOH (0.5 M) (pH=11–12). Blue-colored block-shaped crystals (43.1 mg, 9.78×10^{-2} mmol), obtained after the mixture was kept several days without stirring at room temperature, were collected in 49% yield. Anal. Calcd. for $C_{18}H_{16}CuN_4O_5$: C, 50.06; H, 3.73; N, 12.97%. Found: C, 50.20; H, 3.38; N, 12.76%.

2.5. Synthesis of $[Cu(HMBimc^T)_2]\cdot 2THF\cdot H_2O$ (**3**$\cdot 2THF\cdot H_2O$)

A solution of $Cu(ClO_4)_2\cdot 6H_2O$ (73.3 mg, 0.20 mmol) in EtOH (5 mL) was slowly layered on top of THF (8 mL, middle), and an aqueous solution (5 mL, bottom) of H_2MBimc (44.1 mg, 0.25 mmol) and KOH (0.5 M) (pH=8–9). Purple-colored crystals (28.5 mg, 4.95×10^{-2} mmol), obtained after the mixture was kept two weeks without stirring at room temperature, were collected in 35% yield. Anal. Calcd. for $C_{22}H_{24}CuN_4O_6$ (**3**$\cdot THF\cdot H_2O$): C, 52.43; H, 4.80; N, 11.12%. Found: C, 52.37; H, 5.02; N, 10.76%.

2.6. X-ray crystallography

Suitable single crystals of **1a**$\cdot 3.5H_2O\cdot EtOH$, **1b**, **2**$\cdot 1/2H_2O$, and **3**$\cdot 2THF\cdot H_2O$ were selected for indexing and the collection of intensity data. Measurements were performed using graphite-monochromatized Mo Kα radiation (λ=0.71073 Å) on a Bruker Smart Apex CCD diffractometer for **1a**$\cdot 3.5H_2O\cdot EtOH$ and on a Bruker Smart CCD diffractometer for **1b**, **2**$\cdot 1/2H_2O$, and **3**$\cdot 2THF\cdot H_2O$. Intensity data were collected at 150(1) K within the limits $1.71^\circ<\theta<27.50^\circ$ for **1a**$\cdot 3.5H_2O\cdot EtOH$, at 296(2) K within the limits $1.76^\circ<\theta<25.01^\circ$ for **1b**, at 293(2) K within the limits $1.42^\circ<\theta<27.52^\circ$ for **2**$\cdot 1/2H_2O$, and at 150(2) K within the limits $1.41^\circ<\theta<25.02^\circ$ for **3**$\cdot 2THF\cdot H_2O$. The structures were solved by direct methods and refined by full-matrix least-squares method on F^2 using the SHELX-97 [21] program packages. Anisotropical thermal factors were assigned to non-hydrogen atoms. The C–H hydrogen atoms were assigned by geometrical calculation and refined as a

Table 1
Crystallographic data for **1a**$\cdot 3.5H_2O\cdot EtOH$, **1b**, **2**$\cdot 1/2H_2O$, and **3**$\cdot 2THF\cdot H_2O$.

	1a$\cdot 3.5H_2O\cdot EtOH$	**1b**	**2**$\cdot 1/2H_2O$	**3**$\cdot 2THF\cdot H_2O$
Empirical formula	$C_{18}H_{25}CdN_4O_{9.50}$	$C_{16}H_{12}CdN_4O_5$	$C_{18}H_{17}CuN_4O_{5.50}$	$C_{26}H_{32}CuN_4O_7$
fw	561.82	452.70	440.90	576.10
Crystal system	Triclinic	Monoclinic	Monoclinic	Monoclinic
Space group	$P\bar{1}$	$C2/c$	$P2_1/c$	$P2_1/c$
a (Å)	9.2301(8)	24.2997(18)	14.7996(9)	15.6668(4)
b (Å)	10.0916(8)	8.9285(7)	8.8387(5)	12.0204(3)
c (Å)	13.0872(11)	15.1958(12)	13.8202(7)	15.4503(3)
α (deg.)	108.078(2)	90	90	90
β (deg.)	102.556(2)	107.665(2)	104.601(3)	112.6510(10)
γ (deg.)	99.308(2)	90	90	90
V (Å^3)	1096.08(16)	3141.4(4)	1749.43(17)	2685.19(11)
Z	2	8	4	4
T (K)	150(1)	296(2)	293(2)	150(2)
λ (Å)	0.71073	0.71073	0.71073	0.71073
D_c (g cm^{-3})	1.705	1.914	1.674	1.425
F(0 0 0)	572	1792	904	1204
μ (mm^{-1})	1.057	1.429	1.293	0.865
R_1[a], WR_2[b] [$I>2\sigma(I)$]	0.0569, 0.1057	0.0280, 0.0597	0.0492, 0.1080	0.0436, 0.1127
R_1[a], WR_2[b] (all data)	0.0828, 0.1137	0.0406, 0.0641	0.1088, 0.1276	0.0659, 0.1324
GooF	1.046	1.044	0.998	1.074
Largest peak/hole (e Å^{-3})	1.058, −1.256	0.414, −0.352	0.418, −0.464	0.647, −0.421

[a] $R_1=\sum||F_o|-|F_c||/\sum|F_o|$.
[b] $WR_2=\{\sum[W(F_o^2-F_c^2)^2]/\sum[W(F_o^2)^2]\}^{1/2}$.

riding model while the O−H and N−H hydrogen atoms were located from the difference in Fourier maps. Experimental details for X-ray data collection and the refinements of **1a** · $3.5H_2O$ · EtOH, **1b**, **2** · $1/2H_2O$, and **3** · 2THF · H_2O are presented in Table 1. CCDC 676609 (**1a** · $3.5H_2O$ · EtOH), 717698 (**1b**), 717699 (**2** · $1/2H_2O$), and 717700 (**3** · 2THF · H_2O) contain the supplementary crystallographic data for this paper. These data can be obtained free of charge from the Cambridge Crystallographic Data Center via www.ccdc.cam.ac.uk/data_request/cif.

3. Results and discussion

3.1. Preparation

The Cd(HBimc)-based metal–organic coordination polymer [Cd(HBimc^N)(HBimc^T)(H_2O)] · $3.5H_2O$ · EtOH (**1a** · $3.5H_2O$ · EtOH, H_2Bimc = 1*H*-benzimidazole-5-carboxylic acid) was prepared by diffusion of an ethanol solution of $Cd(ClO_4)_2 \cdot 6H_2O$ into an aqueous solution of H_2Bimc and KOH at 4 °C (Scheme 2), while the compound [Cd(HBimc^N)(HBimc^T)(H_2O)] (**1b**) was hydrothermally synthesized at 150 °C using $CdCl_2 \cdot 2.5H_2O$, H_2Bimc, and 1,4-diaza-bicyclo [2,2,2] octane (DABCO) as the starting materials.

Following a similar procedure to that for **1a**, the Cu(HMBimc)-based metal–organic coordination polymers, [Cu(HMBimc^N)$_2$(H_2O)] · $1/2H_2O$ (**2** · $1/2H_2O$, H_2MBimc = 2-methyl-1*H*-benzimidazole-5-carboxylic acid) and [Cu(HMBimc^T)$_2$] · 2THF · H_2O (**3** · 2THF · H_2O), were also prepared. Both **2** · $1/2H_2O$ and **3** · 2THF · H_2O formed crystals at room temperature from the self-assembly reactions of $Cu(ClO_4)_2 \cdot 6H_2O$ and H_2MBimc in C_2H_5OH/THF/H_2O solvent systems, but with varying metal-to-ligand ratios (*M*:*L* = 2:5 for **2** and 4:5 for **3**).

3.2. Cd(HBimc)-based coordination polymers

The molecular structures of Cd(HBimc)-based coordination polymers **1a** and **1b** were determined. Single-crystal X-ray diffraction analyses revealed that both **1a** and **1b** are supramolecular isomers [22]. These isomers have the same formula [Cd(HBimc^N)(HBimc^T)(H_2O)], but their networks are structurally different. The most striking result of the present study is that a pair of tautomeric HBimc building blocks, namely the normal (***N*** or HBimc^N) and tautomer (***T*** or HBimc^T) configurations of HBimc (Scheme 1), has quite different bonding characteristics, but is simultaneously included in the structures of **1a** and **1b**. The coordination of HBimc^N (***N***-configuration) is 3,5-bridged as follows: the carboxylate in the 5-position is connected to a 3-coordinated benzimidazole moiety. In contrast, the ***T***-configuration (HBimc^T) exhibits 1,5-bridging as follows: the carboxylate in the 5-position is bonded to a benzimidazole moiety donated from the 1-position. The benzimidazole-NH proton shifts from the 1- to

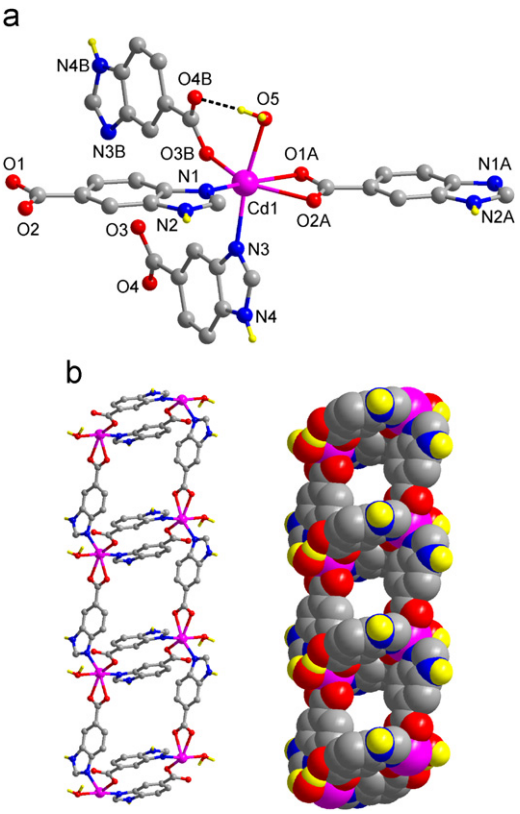

Fig. 1. (a) Local connectivity around the Cd^{II} center in **1a**. (b) The ladder-like chain structure of **1a** as represented by both ball-and-stick and space-filling models. Color scheme: pink, Cd; red, O; blue, N; gray, C; yellow, H. Black dashed line refers to intramolecular OH···O hydrogen-bond. (For interpretation of the references to color in this figure legend, the reader is referred to the web version of this article.)

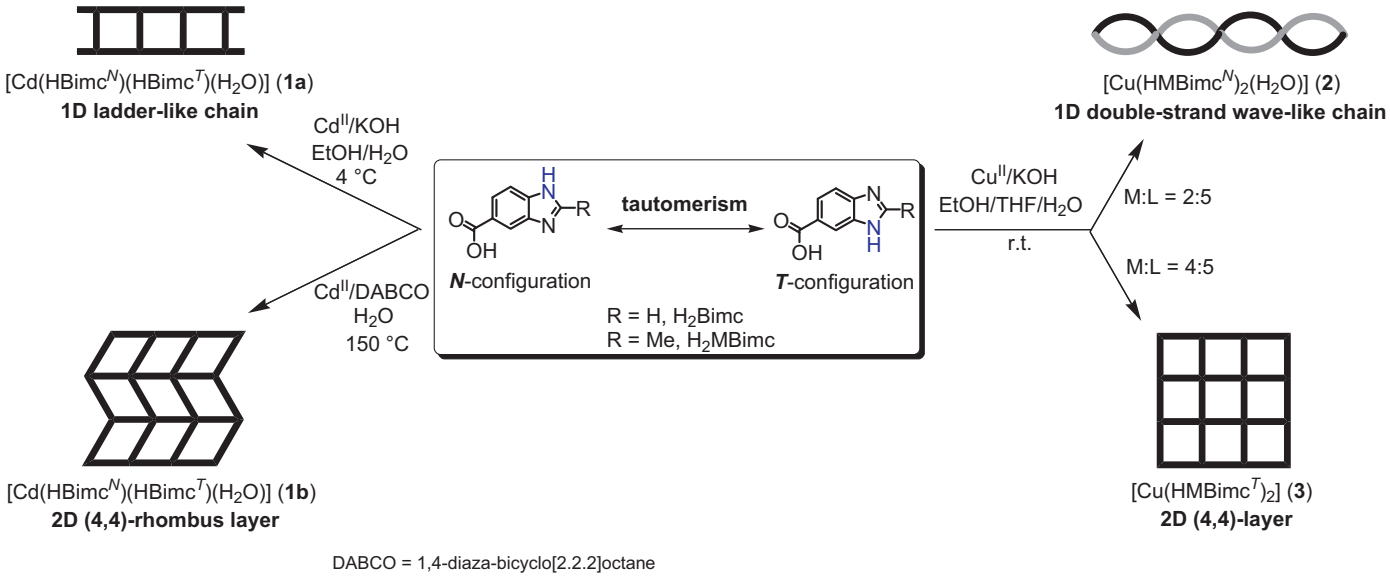

Scheme 2. Syntheses of **1**–**3**.

the 3-position as the result of the inherent delocalized nature of the heterocyclic benzimidazole moiety. This finding demonstrates that H_2Bimc is tautomerized through polar-solvent-mediated (H_2O, MeOH, and/or EtOH) proton-shuttling during the self-assembly process [23]. Nevertheless, the possibility that both tautomers of H_2Bimc are simultaneously present in solution cannot be excluded.

Solid state structural analysis reveals that the Cd^{II} ions in **1a** exhibit a distorted octahedral geometry consisting of two *cis*-coordinated benzimidazole nitrogen (N_{Bim}) atoms (Cd–N_{Bim}, 2.271(4)–2.285(4) Å), three carboxylate oxygen (O_{COO^-}) atoms (Cd–O_{COO^-}, 2.241(3)–2.387(3) Å), and one water molecule (Cd–OH_2, 2.356(4) Å), as shown in Fig. 1a. The coordinated water molecule (O5) is intramolecularly hydrogen bonded (O···O=2.68 Å, OH···O=174°, Table 2) to the noncoordinated carboxylate oxygen (O4) of the HBimc ligand. Compound **1a** adopts an infinite 1D ladder-like chain structure (Fig. 1b), constructed from two distinct types of building subunits: the hydrogen-bond-stabilized M_2L_2-metallocyclic stair and the 1D straight $-(M-L)_n-$ edge (Fig. S1). The carboxylate groups in the ***N***- and ***T***-configured HBimc ligands exhibit monodentate and chelating bidentate coordination modes, respectively. As a result of inter-ladder $\pi-\pi$ interactions (centroid^{Im}···centroid^{Ph} distance= 3.62 Å) between the benzimidazole rings and OH···O hydrogen-bonding interactions (O···O=2.70 Å) and between coordinated water molecules (O5) and chelated carboxylate (O2) groups, a 3D supramolecular structure is achieved (Fig. 2).

In **1b**, the coordination environment around the Cd^{II} ion is nearly identical to that in **1a**: two *cis*-coordinated N_{Bim} atoms (Cd–N_{Bim}, 2.282(3)–2.290(3) Å), three O_{COO^-} atoms (Cd–O_{COO^-}, 2.227(2)–2.515(2) Å), and one water molecule (Cd–OH_2, 2.359(2) Å) (Fig. 3a). Intramolecular OH···O hydrogen bonds (O···O=2.67 Å, Table 1) between the coordinated water molecule (O5) and the carboxylate group (O2) of the HBimc ligand and NH···O (N···O=2.89 Å) between benzimidazole (N4) groups and the coordinated water molecule (O5) are present. Compound **1b** adopts a 2D (4,4)-rhombus layer structure, as shown in Fig. 3b. The layer structure is intercrossed by two subunit types comprised of 1D $-(M-L)_n-$ chains (Fig. S2), both of which are formed from Cd^{II} ions and HBimc ligands, but the HBimc ligand configuration varies, i.e. ***N***- and ***T***-configurations. The carboxylate

Table 2
Hydrogen bonding parameters in **1a**•3.5H_2O•EtOH, **1b**, **2**•1/2H_2O, and **3**•2THF•H_2O (D, Donor atom; A, Acceptor atom).

D–H···A	D–H•(Å)	H···A (Å)	D···A (Å)	D–H···A (°)	Symmetry code
1a•3.5H_2O•EtOH					
N(2)–H(2A)···O(6)	0.88	1.98	2.82	159	$x, 1+y, 1+z$
N(4)–H(4B)···O(7)	0.88	1.92	2.77	162	$1-x, -y, 1-z$
O(5)–H(5A)···O(4)	0.90	1.78	2.68	174	$2-x, -y, 1-z$
O(5)–H(5B)···O(2)	0.90	1.84	2.70	161	$2-x, 1-y, 2-z$
O(6)–H(6B)···O(4)	0.90	1.86	2.76	174	x, y, z
O(7)–H(7A)···O(3)	0.90	2.09	2.91	150	x, y, z
O(8)–H(8B)···O(1)	0.94	2.16	2.95	142	$2-x, 1-y, 1-z$
O(9)–H(9B)···O(5)	0.90	2.35	3.21	161	$-1+x, y, z$
O(9)–H(9C)···O(8)	0.95	1.93	2.81	153	$x, y, 1+z$
1b					
N(1)–H(101)···O(4)	0.94	2.01	2.93	166	$-x, 1+y, 1/2-z$
N(4)–H(102)···O(5)	0.95	2.03	2.89	148	$x, -y, 1/2+z$
O(5)–H(103)···O(2)	0.91	1.84	2.67	149	x, y, z
O(5)–H(104)···O(3)	0.87	1.92	2.77	164	$1/2-x, -1/2-y, 1-z$
2•1/2H_2O					
N(1)–H(101)···O(2)	0.89	1.94	2.80	163	$x, 1/2-y, 1/2+z$
N(3)–H(102)···O(6)	0.87	2.14	2.91	147	$-x, 1-y, -z$
O(5)–H(103)···O(2)	0.86	2.29	3.08	153	$1-x, 1-y, -z$
O(5)–H(104)···O(2)	0.89	1.84	2.69	160	x, y, z
O(6)–H(105)···O(4)	0.84	2.45	2.85	110	x, y, z
O(6)–H(106)···O(4)	0.85	2.04	2.67	131	$-x, 2-y, -z$
3•2THF•H_2O					
N(2)–H(101)···O(7)	0.87	1.85	2.71	168	$-x, -1/2+y, 1/2-z$
N(4)–H(102)···O(2)	0.84	1.94	2.76	164	$1-x, 1-y, 1-z$
O(7)–H(103)···O(5)	0.93	1.84	2.74	160	$x, 1+y, z$
O(7)–H(104)···O(4)	0.90	1.80	2.70	173	x, y, z

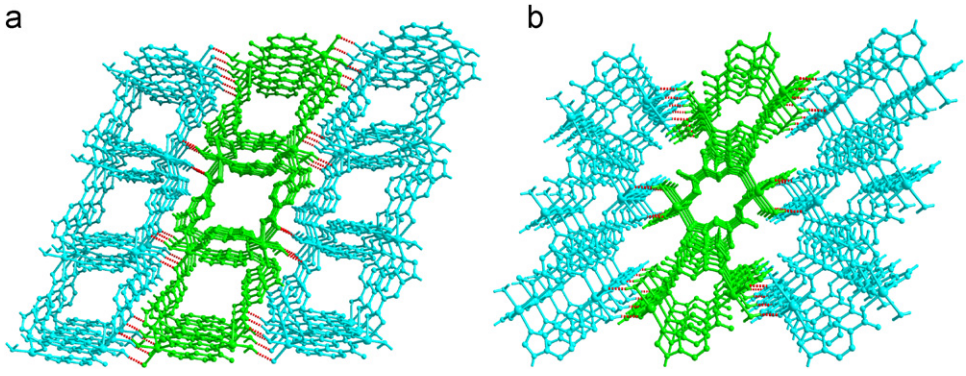

Fig. 2. Projection view of packing diagram for **1a** along the crystallographic (a) *a*- and (b) *b*-axes. Red dashed lines refer to intermolecular hydrogen bonds. (For interpretation of the references to color in this figure legend, the reader is referred to the web version of this article.)

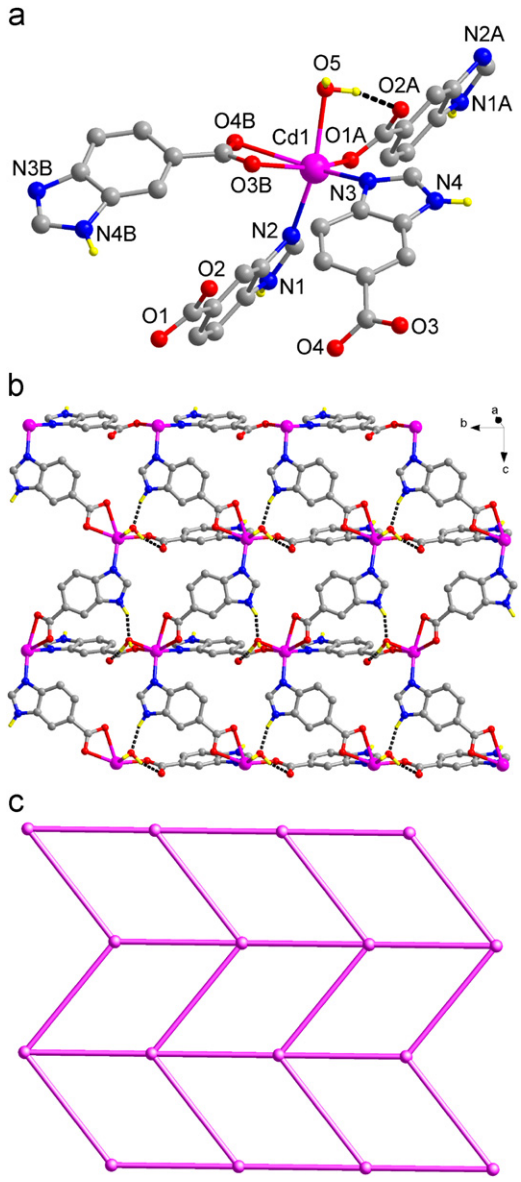

Fig. 3. (a) Local connectivity around the Cd^{II} center in **1b**. (b) Ball-and-stick and (c) schematic representations of the Cd-based 2D (4,4)-rhombus layer structure of **1b**. Color scheme: pink, Cd; red, O; blue, N; gray, C; yellow, H. Black dashed lines refer to intramolecular OH···O and intra-layer NH···O hydrogen bonds. (For interpretation of the references to color in this figure legend, the reader is referred to the web version of this article.)

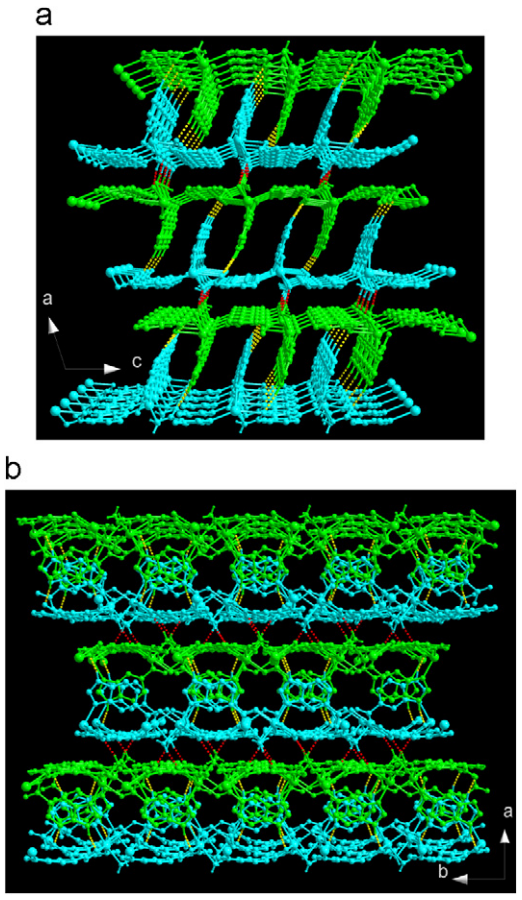

Fig. 4. Projection view of packing diagram for **1b** along the crystallographic (a) *b*- and (b) *c*-axes. Through inter-wall OH···O hydrogen-bonding interactions (red dashed lines), the interlaced wall-like layer architecture, stabilized by inter-layer NH···O hydrogen-bonds (yellow dashed lines) and $\pi-\pi$ interactions (not shown), leads to the formation of a 3D supramolecular network. (For interpretation of the references to color in this figure legend, the reader is referred to the web version of this article.)

groups exhibit a monodentate in the $HBimc^N$ ligands and a bidentate chelating mode in the $HBimc^T$ ligands. As a result of inter-layer $\pi-\pi$ stacking interactions ($centroid^{Im}\cdots centroid^{Ph}$ distance = 3.80 and 3.82 Å) between adjacent benzimidazole rings of the ***N***-configured HBimc ligands in two neighboring layers and NH···O hydrogen-bonding interactions (N···O = 2.93 Å) between the benzimidazole (N1) groups and chelated carboxylate (O4) groups, an interlaced double-layer wall-like structure is formed (Fig. S3). This double-layer wall-like structure permits the extensions of a 3D network through inter-wall OH···O hydrogen bonds (O···O = 2.77 Å) between coordinated water molecules (O5) and chelated carboxylate (O3) groups (Fig. 4). A PLATON [24] analysis suggests the absence of a solvent-accessible-void volume.

It is noteworthy that in **1a** and **1b**, the four HBimc ligands around the Cd^{II} center exhibit different bridging orientations, presumably due to the instinctive free rotations of the $Cd-N_{Bim}$ and the $C_{Bim}-O_{COO^-}$ bonds. In **1a**, the two $HBimc^T$ ligands show a linear *exo*-bridging configuration and the two $HBimc^N$ ligands exhibit *pseudoendo*-bridged characteristics (Fig. 1a), but in **1b**, the two $HBimc^T$ ligands are in a bent *exo*-bridging configuration and the two $HBimc^N$ ligands are in a linear *exo*-bridging configuration (Fig. 3a). These bridging characteristics, which allow bond formation with further metal centers, lead to the formation of supramolecular isomers **1a** and **1b**.

To date, although several Cd(HBimc)-based metal–organic coordination networks have been reported [15,16,17b], the unique properties in the bonding characteristic changes in the proton-shuttled ligands and their influence in extended architectures have been of minor concern and have not yet been systematically addressed. Table 3 summarizes these results together with Co- [16], Mn- [17a], Ni- [15c], and Cu-analogs (this work). The molecular components (formula) of all of these products are quite similar, but their crystal structures vary. This could be due to the influence of the diverse multifunctional coordination sites, flexibility along the C_{Bim}–$C_{carboxylate}$ single bond, the various pH-controlled coordination modes, and most important, the self-modulated proton-shuttling capability of the HBimc ligand.

3.3. Cu(HMBimc)-based coordination polymers

A single-crystal X-ray diffraction analysis reveals that compound $[Cu(HMBimc)_2(H_2O)]\cdot 1/2H_2O$ ($\mathbf{2}\cdot 1/2H_2O$) crystallizes in the monoclinic space group $P2_1/c$. Pentacoordinated Cu^{II} ions possess a square pyramidal geometry ($\tau = 0.195$) [25] of

Table 3
Summary of the structural features of HBimc and HMBimc ligands in metal–organic coordination networks.

Compounds	Configurations of ligands	Coordination networks	Ref.
$[Cd(HBimc^{N})(HBimc^{T})(H_2O)]\cdot 3.5H_2O\cdot EtOH$ (**1a**$\cdot 3.5H_2O\cdot EtOH$)	***N***- and ***T***-configurations	1D ladder	This work
$[Cd(HBimc^{N})(HBimc^{T})(H_2O)]$ (**1b**)	***N***- and ***T***-configurations	2D (4,4)-rhombus net	This work
$[Cd(HBimc^{N})(HBimc^{T})(H_2O)]\cdot 2CH_3OH$	***N***- and ***T***-configurations	2D (4,4)-layer	16
$[Cd(HBimc^{N})(HBimc^{T})(H_2O)]\cdot$4,4'-bpy$\cdot H_2O$	***N***- and ***T***-configurations	2D (4,4)-layer	15b
$[Cd(HBimc^{N})(HBimc^{T})]$	***N***- and ***T***-configurations	2D (4,4)-rhombus net	15a,17b
$[Cd(HBimc^{N})(HBimc^{T})]\cdot H_2O$	***N***- and ***T***-configurations	3D network	15a
$[Cd(HBimc^{N})_2(H_2O)_2]\cdot 2H_2O$	***N***-configuration only	1D double-strand wave-like chain	15a
$[Mn(HBimc^{N})_2(H_2O)_2]\cdot 2H_2O$	***N***-configuration only	1D double-strand wave-like chain	17a
$[Co(HBimc^{N})_2(H_2O)_2]\cdot 2H_2O$	***N***-configuration only	1D double-strand wave-like chain	16
$[Ni(HBimc^{N})(HBimc^{T})]$	***N***- and ***T***-configurations	2D (4,4)-rhombus net	15c
$[Cu(HMBimc^{N})_2(H_2O)]\cdot 1/2H_2O$ (**2**$\cdot 1/2H_2O$)	***N***-configuration only	1D double-strand wave-like chain	This work
$[Cu(HMBimc^{T})_2]\cdot 2THF\cdot H_2O$ (**3**$\cdot 2THF\cdot H_2O$)	***T***-configuration only	2D (4,4)-layer	This work

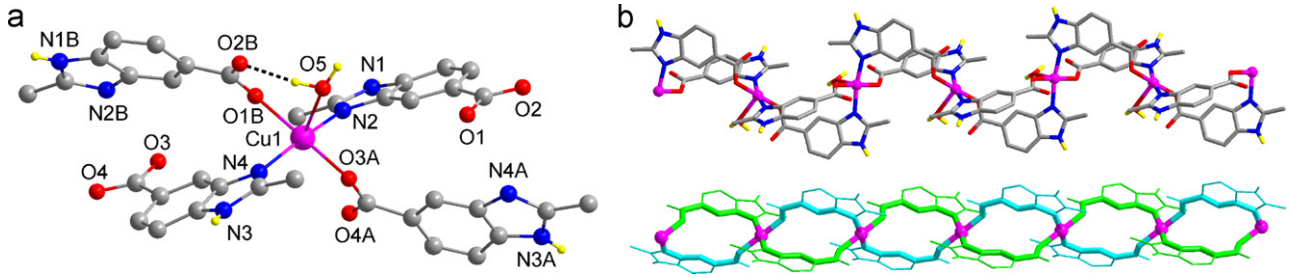

Fig. 5. (a) Local connectivity around the Cu^{II} center in **2**. Color scheme: cyan, Cd; red, O; blue, N; gray, C; yellow, H. Black dashed line refers to intramolecular OH···O hydrogen-bond. (b) Double-stranded wave-like chain structure of **2** (upper); the two single-stranded wave-like chains are represented in cyan and green (lower), respectively. (For interpretation of the references to color in this figure legend, the reader is referred to the web version of this article.)

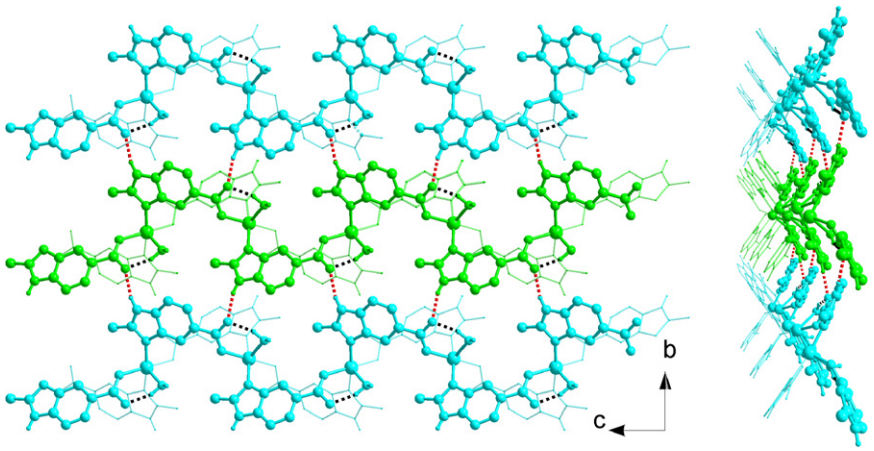

Fig. 6. Top-view (left) and side-view (right) of the 2D sheet structure in the *bc*-plane in **2**, constructed by inter-chain NH···O_{COO^-} H-bonding interactions (red-dashed lines). Black dashed lines refer to intramolecular OH···O_{COO^-} H-bonding interactions. (For interpretation of the references to color in this figure legend, the reader is referred to the web version of this article.)

$CuN_2O_2(H_2O)$ comprised of two N_{Bim} (Cu–N_{Bim}, 1.965(3)–1.966(3) Å) and two O_{COO^-} atoms (Cu–O_{COO^-}, 1.947(3)–2.003(2) Å) from four HMBimc units in a *trans,trans*-conformation at the basal plane and one water molecule (Cu–OH_2, 2.439(3) Å) at the apical position (Fig. 5a). The coordinated water (O5) molecules interact with the noncoordinated carboxylate oxygen (O2) atoms of HMBimc ligands through intramolecular hydrogen bonds (O···O=2.69 Å, Table 2). The HMBimc ligand shows only the ***N***-configured coordinated structure to bridge two Cu^{II} ions through a benzimidazole moiety and a monodentate carboxylate group. Compound **2** adopts a 1D double-stranded wave-like chain architecture, in which two single-stranded wave-like chains intersect with each other at the Cu^{II} centers in a head-to-tail manner (Fig. 5b). This structure is closely analogous to compounds $[M(HBimc^{N})_2(H_2O)_2]$ (M=Cd, Co, Mn) [15a,16,17a].

Although **2** and the $[M(HBimc^{N})_2(H_2O)_2]$-analog (M=Cd, Co, Mn) [15a,16,17a] have nearly identical metal–ligand directed 1D double-stranded wave-like chain structures, the crystal packing for the two are slightly different, which most likely can be attributed to the influence of the methyl substitutent. In **2**, each double-strand wave-like chain hydrogen-bonded to neighboring chains via inter-chain NH···O interactions (N···O=2.80 Å) between the benzimidazole (N1) moieties and the monodentate carboxylate (O2) groups gives rise to a 2D sheet structure in the *bc*-plane (Fig. 6). These sheets are arranged in an ABAB order along the crystallographic *a*-axis with different inter-sheet separations (Fig. 7). One contains no guest

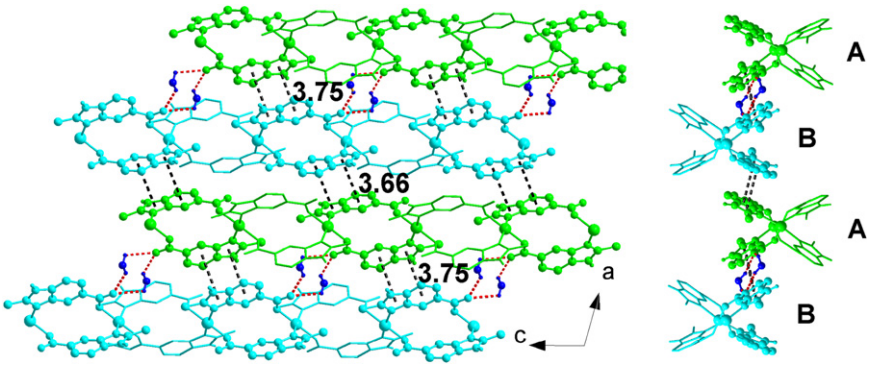

Fig. 7. Top-view (left) and side-view (right) of the $\pi-\pi$ stacking interactions assisted 2D sheet structure in the *ac*-plane in **2**. Red and black dashed lines refer to OH···O_{COO^-} H-bonding interactions and $\pi-\pi$ stacking interactions, respectively. (For interpretation of the references to color in this figure legend, the reader is referred to the web version of this article.)

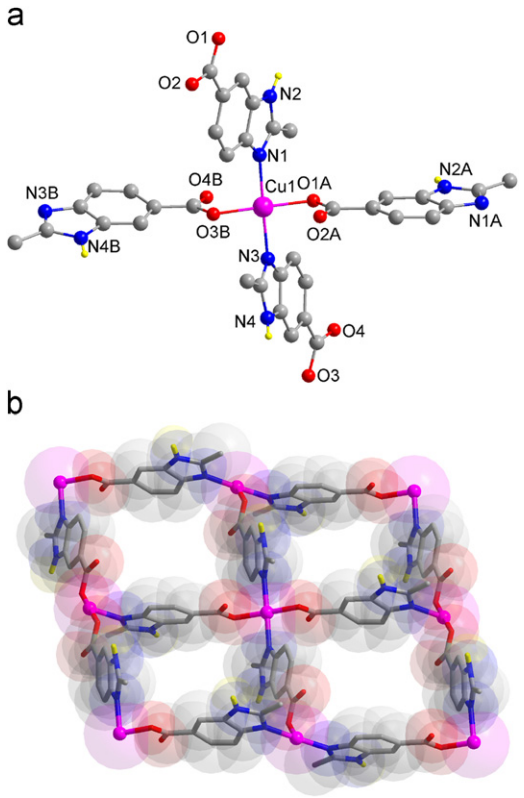

Fig. 8. (a) Local connectivity around the Cu^{II} center in **3**. (b) Space-filling model superimposed on a wire/stick representation of the (4,4)-topological layer structure of **3**. Color scheme: pink, Cu; red, O; blue, N; gray, C; yellow, H. (For interpretation of the references to color in this figure legend, the reader is referred to the web version of this article.)

molecules and shows OH···O interactions (O···O = 3.08 Å) between the coordinated water (O5) molecules and the monodentate carboxylate (O2) groups in neighboring sheets and $\pi-\pi$ stacking interactions (centroid^{im}···centroid^{ph} distance = 3.66 Å) between the benzimidazole rings of the $HMBimc^{N}$ ligands. The other includes guest water (O6) molecules that are hydrogen bonded to the monodentate carboxylate (O4) groups in adjacent sheets and exhibits $\pi-\pi$ stacking interactions (centroid^{im}···centroid^{ph} distance = 3.75 Å) between the benzimidazole rings of another set of ***N***-configured HMBimc ligands. As a consequence, these noncovalent interactions, including NH···O, OH···O, and $\pi-\pi$ interactions, support an extensive 3D architecture (Fig. S4).

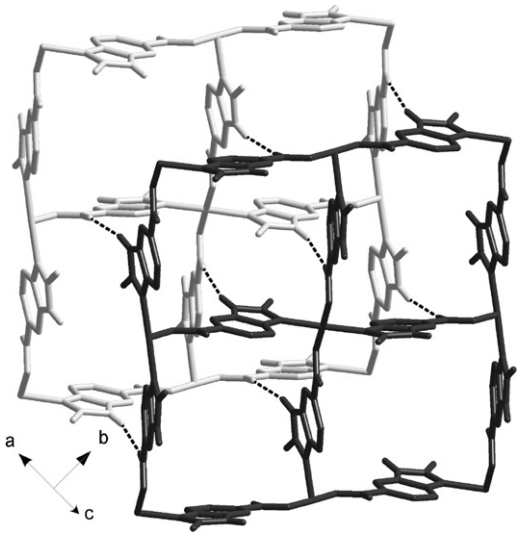

Fig. 9. The NH···O hydrogen bond-supported bi-layer structure in **3**.

Compound $[Cu(HMBimc)_2]\cdot 2THF\cdot H_2O$ (**3**·2THF·H_2O) crystallizes in the monoclinic space group $P2_1/c$. Two *trans*-coordinated N_{Bim} atoms (Cu–N_{Bim}, 1.975(3)–1.982(3) Å) and two *trans*-coordinated O_{COO^-} atoms (Cu–O_{COO^-}, 1.959(2)–1.964(2) Å) surround the Cu^{II} ions, leading to a square planar geometry (Fig. 8a). Compound **3** adopts a 2D (4,4)-topological layered structure (Fig. 8b), in which the layer is intercrossed by subunits of 1D –$(M-L)_n$– chains, formed by Cu^{II} ions and ***T***-configured HMBimc ligands (Fig. S5). As a result of NH···O hydrogen-bonding interactions (N···O = 2.76 Å, Table 2) between the benzimidazole (N4) groups and carboxylate (O2) groups, a H-bonded bi-layer structure is formed (Fig. 9). When viewed along the crystallographic *a*-axis, 1D rectangular channels with effective dimensions of approximately 4.5×6.7 Å^2 are observed. A PLATON [24] analysis suggests a solvent-accessible-void volume of 1212.3 Å^3 (45.1% of the unit cell volume), in which the lattice THF and water molecules reside (Fig. 10).

Structural analyses of many metal–organic networks have shown that multicarboxylate ligands may be present as two or more coordination configurations in the structures [26,27]. However, these ligands do not possess tautomeric characteristics. Imidazolecarboxylate-based ligands exhibit different coordination modes in different compounds [5–18]. While it is unusual to observe more than two coordination modes in the same structure [7c], this is not the case for tautomeric configurations. Herein, the two benzimidazolecarboxylate derivatives, HBimc and HMBimc, are unique and have an asymmetric molecular architecture with resonated tautomeric forms that result

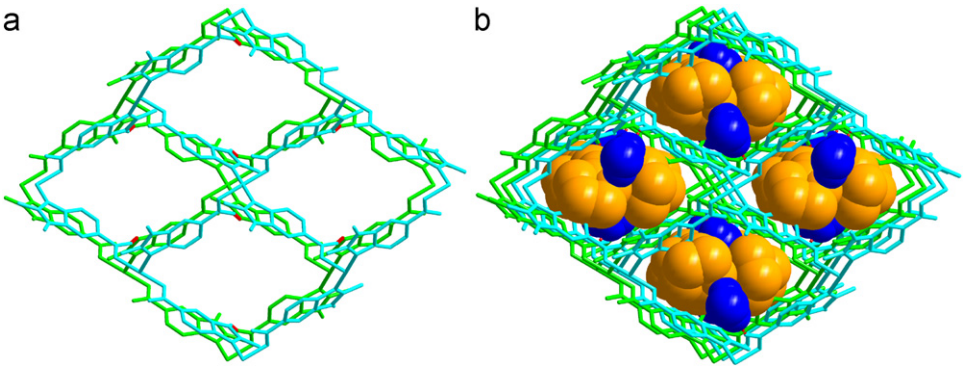

Fig. 10. (a) The packing diagram of **3**•2THF•H_2O along the crystallographic *a*-axis showing the 1D rectangular channels. (b) Guest THF (orange space-filling model) and water (blue space-filling model) molecules inside the 1D rectangular channels. Red dashed lines refer to NH···O hydrogen-bonding interactions. (For interpretation of the references to color in this figure legend, the reader is referred to the web version of this article.)

from double-bond conjugation and proton shuttling. As a consequence, compounds **1a** and **1b** together with [Cd(HBimc^N)(HBimc^T)(H_2O)]·2CH_3OH [16] and [Cd(HBimc^N)(HBimc^T)(H_2O)]·4,4′-bpy·H_2O [15b], as well as [Cd(HBimc^N)(HBimc^T)] [15a,17b], [Cd(HBimc^N)(HBimc^T)]·H_2O [15a], and [Ni(HBimc^N)(HBimc^T)] [15c], represent extremely attractive cases of the simultaneous inclusion of a pair of tautomeric normal (***N*** or HBimc^N) and tautomer (***T*** or HBimc^T)-configured 1*H*-benzimidazole-5-carboxylate building blocks in the structures. On the other hand, it is particularly noteworthy that the HMBimc ligand shows only the ***N***-configuration in **2** and only the ***T***-configuration in **3** (Table 3). Both configurations of the HMBimc ligand are individually present in the two distinct structures **2** and **3**, which are produced from the same reactants and solvent systems with the only difference being the metal-to-ligand ratios used. It is likely that spontaneous proton transfer occurred during the self-assembly process, although the possibility that both tautomers of H_2MBimc, ***N*** and ***T***-modes, are present in solution cannot be excluded. The isolation of a metal–organic network **3** possessing only a tautomer (***T***) mode of tautomeric benzimidazolecarboxylate-based ligand is fascinating.

3.4. Thermal properties

Thermogravimetric (TG) analyses of **1**–**3** were performed on polycrystalline samples, which were treated under vacuum before the TG measurements, under a nitrogen atmosphere (Fig. S9). **1a**·3.5H_2O exhibited a gradual weight-loss trace as the free and coordinated water molecules were released (found 15.4%, calcd. 15.7%) upon heating to 135 °C, and then decomposed at temperatures greater than 367 °C. Sample **1b** showed the release of coordinated water molecules (found 3.7%, calcd. 4.0%) in the temperature range from 140 to 190 °C. Before decomposition, the species is thermally stable up to a temperature of approximately 345 °C. For **2**·1/2H_2O; the lattice water molecules are removed from room temperature for up to 95 °C (found 2.1%, calcd. 2.0%); the framework then begins to decompose on approaching 300 °C. Analysis of the TG trace of **3** revealed that an approximately 3.0% weight-loss occurred in the temperature range from room temperature to 90 °C, as the result of the evaporation of trace amounts of free water molecules (3.2%). The main structure of **3** was maintained and then it began to decompose at temperatures greater than 270 °C.

3.5. Photoluminescent properties

The photoluminescent properties of the free HBimc ligand and the Cd(HBimc)-based coordination polymer **1b** in the solid state were investigated at room temperature and relevant emission spectra are shown in Fig. S10. Upon excitation at 310 nm, the free HBimc ligand shows an intense emission band centered at 345 nm and a very weak emission band around 555 nm. In contrast, compound **1b** exhibits an emission band at 384 nm with three weak shoulders at 437, 490, and 547 nm when irradiated at 310 nm. The distinct red-shift in the emission of **1b**, compared to the HBimc ligand, may be attributed to the cooperative effect of intraligand and ligand-to-metal charge transfer (LMCT) transitions [15a,16].

4. Conclusion

This work presents some fascinating cases in that the tautomeric building blocks (***N***- and ***T***-configurations) of the benzimidazolecarboxylate ligands, H_2Bimc and H_2MBimc, are simultaneously included or individually present in the structures of cadmium(II) and copper(II) coordination polymers. Of particular interest is the existence of only a tautomer (***T***) mode of the benzimidazolecarboxylate-based ligand in a copper(II) network, which is observed for the first time.

Acknowledgments

We thank the Academia Sinica and the National Science Council of Taiwan for financial support.

Appendix A. Supporting information

Supporting information containing further structure diagrams for **1b**, **2**, and **3**, IR spectrum and PXRD patterns of **1b**, thermogravimetric (TG) curves, and photoluminescence spectra is available on the Web under http://www.sciencedirect.com or from the authors.

Supporting information associated with this article can be found in the online version at doi:10.1016/j.jssc.2011.05.002.

References

[1] [a] B.F. Abrahams, M.G. Haywood, R. Robson, D.A. Slizys, Angew. Chem. Int. Ed. 42 (2003) 1111;
[b] M.J. Zaworotko, Nature 451 (2008) 410;
[c] R. Banerjee, A. Phan, B. Wang, C. Knobler, H. Furukawa, M. O'Keeffe, O.M. Yaghi, Science 319 (2008) 939;
[d] K. Sanderson, Nature 448 (2007) 746;
[e] A.K. Cheetham, C.N.R. Rao, Science 318 (2007) 58;
[f] S. Kitagawa, Nature 441 (2006) 584;
[g] J.T. Hupp, K.R. Poeppelmeier, Science 309 (2005) 2008.

[2] [a] G. Férey, Chem. Soc. Rev. 37 (2008) 191;
[b] D. Bradshaw, J.B. Claridge, E.J. Cussen, T.J. Prior, M.J. Rosseinsky, Acc. Chem. Res. 38 (2005) 273;
[c] M.W. Hosseini, Acc. Chem. Res. 38 (2005) 313.
[3] [a] S.S. Han, W.-Q. Deng, W.A. Goddard III, Angew. Chem. Int. Ed. 46 (2007) 6289;
[b] R.J. Hill, D.-L. Long, N.R. Champness, P. Hubberstey, M. Schröder, Acc. Chem. Res. 38 (2005) 337;
[c] M. Fujita, M. Tominaga, A. Hori, B. Therrien, Acc. Chem. Res. 38 (2005) 371;
[d] B. Kesanli, W. Lin, Coord. Chem. Rev. 246 (2003) 305;
[e] R.E. Morris, P.S. Wheatley, Angew. Chem. Int. Ed. 47 (2008) 4966;
[f] G.R. Desiraju, Angew. Chem. Int. Ed. 119 (2007) 8492.
[4] [a] J.-Y. Wu, S.-L. Yang, T.-T. Luo, Y.-H. Liu, Y.-W. Cheng, Y.-F. Chen, Y.-S. Wen, L.-G. Lin, K.-L. Lu, Chem. Eur. J. 14 (2008) 7136;
[b] G. Li, W. Yu, Y. Cui, J. Am. Chem. Soc. 130 (2008) 4582;
[c] K. Tanaka, S. Oda, M. Shiro, Chem. Commun. (2008) 820;
[d] J.J. Vittal, Coord. Chem. Rev. 251 (2007) 1781;
[e] C.J. Kepert, Chem. Commun. (2006) 695.
[5] Y.-H. Liu, H.-C. Wu, H.-M. Lin, W.-H. Hou, K.-L. Lu, Chem. Commun. (2003) 60.
[6] M. McCann, M.T. Casey, M. Devereaux, M. Curran, V. McKee, Polyhedron 15 (1996) 2321.
[7] [a] Y.-Q. Sun, J. Zhang, G.-Y. Yang, Chem. Commun. (2006) 1947;
[b] M.-B. Zhang, Y.-M. Chen, S.-T. Zheng, G.-Y. Yang, Eur. J. Inorg. Chem. (2006) 1423;
[c] Y.-Q. Sun, J. Zhang, Y.-M. Chen, G.-Y. Yang, Angew. Chem. Int. Ed. 44 (2005) 5814.
[8] [a] Q. Xu, R.-Q. Zou, R.-Q. Zhong, C. Kachi-Terajima, S. Takamizawa, Cryst. Growth Des. 8 (2008) 2458;
[b] R.-Q. Zou, R.-Q. Zhong, L. Jiang, Y. Yamada, N. Kuriyama, Q. Xu, Chem. Asian J. 1 (2006) 536;
[c] R.-Q. Zou, Y. Yamada, Q. Xu, Micropor. Mesopor. Mater. 91 (2006) 233;
[d] R.-Q. Zou, L. Jiang, H. Senoh, N. Takeichi, Q. Xu, Chem. Commun. (2005) 3526.
[9] T.K. Maji, G. Mostafa, H.-C. Chang, S. Kitagawa, Chem. Commun. (2005) 2436.
[10] Y. Liu, V. Kravtsov, R.D. Walsh, P. Poddar, H. Srikanth, M. Eddaoudi, Chem. Commun. (2004) 2806.
[11] C.-F. Wang, E.-Q. Gao, Z. He, C.-H. Yan, Chem. Commun. (2004) 720.
[12] [a] C. Qin, X. Wang, E. Wang, L. Xu, Inorg. Chem. Commun. 8 (2005) 669;
[b] X. Wang, C. Qin, E. Wang, L. Xu, J. Mol. Struct. 749 (2005) 45.
[13] [a] E. Shimizu, M. Kondo, Y. Fuwa, R.P. Sarker, M. Miyazawa, M. Ueno, T. Naito, K. Maeda, F. Uchida, Inorg. Chem. Commun. 7 (2004) 1191;
[b] M. Kondo, E. Shimizu, T. Horiba, H. Tanaka, Y. Fuwa, K. Nabari, K. Unoura, T. Naito, K. Maeda, F. Uchida, Chem. Lett. 32 (2003) 944.
[14] [a] M.-L. Lehaire, R. Scopelliti, L. Herdeis, K. Polborn, P. Mayer, K. Severin, Inorg. Chem. 43 (2004) 1609;
[b] R.-Q. Fang, X.-M. Zhang, Inorg. Chem. 45 (2006) 4801;
[c] X. Zhang, D. Huang, F. Chen, C. Chen, Q. Liu, Inorg. Chem. Commun. 7 (2004) 662;
[d] B. Zhoa, X.-Q. Zhao, W. Shi, P. Cheng, J. Mol. Struct. 830 (2007) 143;
[e] X.-M. Li, Y.-H. Dong, Q.-W. Wang, B. Liu, Acta Cryst. E 63 (2007) m1274;
[f] X.-F. Zhang, S. Gao, L.-H. Huo, S.W. Ng, Acta Cryst. E 62 (2006) m2860;
[g] X.-F. Lin, Acta Cryst. E 62 (2006) m2039;
[h] Y.-L. Bai, J. Tao, R.-B. Huang, L.-S. Zheng, Acta Cryst. C 61 (2005) m98;
[i] Y. Xu, R.-H. Wang, B.-Y. Lou, L. Han, M.-C. Hong, Acta Cryst. C 60 (2004) m296.
[15] [a] Z. Guo, R. Cao, X. Li, D. Yuan, W. Bi, X. Zhu, Y. Li, Eur. J. Inorg. Chem. (2007) 742;
[b] Z. Guo, X. Li, S. Gao, Y. Li, R. Cao, J. Mol. Struct. 846 (2007) 123;
[c] Z. Guo, D. Yuan, W. Bi, X. Li, R. Cao, J. Mol. Struct. 782 (2006) 106.
[16] Z. Li, Y. Chen, P. Liu, J. Wang, M. Huang, J. Solid State Chem. 178 (2005) 2306.
[17] [a] Q.-J. Deng, M.-H. Zeng, H. Liang, S.W. Ng, K.-L. Huang, Acta Cryst. E 62 (2006) m1293;
[b] Q.-J. Deng, M.-H. Zeng, H. Liang, K.-L. Huang, Chin. J. Struct. Chem. 25 (2006) 975.
[18] [a] Y.-R. Liu, L. Li, T. Yang, X.-W. Yu, C.-Y. Su, CrystEngComm 11 (2009) 2712;
[b] Y. Wei, Y. Yu, R. Sa, Q. Li, K. Wu, CrystEngComm 11 (2009) 1054;
[c] Y.-L. Lo, W.-C. Wang, G.-A. Lee, Y.-H. Liu, Acta Cryst. E 63 (2007) m2657.
[19] M. Du, Z.-H. Zhang, X.-J. Zhao, Q. Xu, Inorg. Chem. 45 (2006) 5785.
[20] [a] Z. Zhou, S. Li, Y. Zhang, M. Liu, W. Li, J. Am. Chem. Soc. 127 (2005) 10824;
[b] S. Li, Z. Zhou, Y. Zhang, M. Liu, Chem. Mater. 17 (2005) 5884;
[c] M. Yamada, I. Honma, Angew. Chem. Int. Ed. 43 (2004) 3688;
[d] M.F.H. Schuster, W.H. Meyer, M. Schuster, K.D. Kreuer, Chem. Mater. 16 (2004) 329;
[e] K.D. Kreuer, A. Fuchs, M. Ise, M. Spaeth, J. Maier, Electrochim. Acta 43 (1998) 1281.
[21] G.M. Sheldrick, SHELX-97 (including SHELXS and SHELXL), University of Göttingen, Göttingen, Germany, 1997.
[22] [a] B.S. Luisi, V.Ch. Kravtsov, B.D. Moulton, Cryst. Growth Des. 6 (2006) 2207;
[b] B. Moulton, M.J. Zaworotko, Chem. Rev. 101 (2001) 1629;
[c] T.L. Hennigar, D.C. MacQuarrie, P. Losier, R.D. Rogers, M.J. Zaworotko, Angew. Chem. Int. Ed. Engl. 36 (1997) 972.
[23] [a] O.-H. Kwon, Y.-S. Lee, H.J. Park, Y. Kim, D.-J. Jang, Angew. Chem. Int. Ed. 43 (2004) 5792;
[b] A.V. Nemukhin, B.L. Grigorenko, I.A. Topol, S.K. Burt, J. Phys. Chem. B 107 (2003) 2958;
[c] K.J. Schweighofer, A. Pohorille, Biophys. J. 78 (2000) 150.
[24] A.L. Spek, PLATON; Utrecht University: Utrecht, the Netherlands, (2000).
[25] A.W. Addison, T.N. Rao, J. Reedijk, J. van Rijn, G.C. Verschoor, J. Chem. Soc., Dalton Trans. (1984) 1349.
[26] [a] J. Wang, Y.-H. Zhang, M.-L. Tong, Chem. Commun. (2006) 3166;
[b] S. Zang, Y. Su, C. Duan, Y. Li, H. Zhu, Q. Meng, Chem. Commun. (2006) 4997;
[c] J.-Y. Wu, T.-T. Yeh, Y.-S. Wen, J. Twu, K.-L. Lu, Cryst. Growth Des. 6 (2006) 467.
[27] [a] L. Cañadillas-Delgado, J. Pasán, O. Fabelo, M. Hernández-Molina, F. Lloret, M. Julve, C. Ruiz-Pérez, Inorg. Chem. 45 (2006) 10585;
[b] H.-F. Zhu, J. Fan, T.-a. Okamura, Z.-H. Zhang, G.-X. Liu, K.-B. Yu, W.-Y. Sun, N. Ueyama, Inorg. Chem. 45 (2006) 3941;
[c] Y.B. Go, X. Wang, E.V. Anokhina, A.J. Jacobson, Inorg. Chem. 44 (2005) 8265;
[d] R. Cao, D. Sun, Y. Liang, M. Hong, K. Tatsumi, Q. Shi, Inorg. Chem. 41 (2002) 2087.